 doi:10.20944/preprints202011.0303.v1

Article

Advanced materials and technologies for compressor blades of small turbofan engines

Dmytro Pavlenko [1]*, Yaroslav Dvirnyk [2] and Radoslaw Przysowa [3]

[1] National University - Zaporizhzhia Polytechnic, Zaporizhzhia, Ukraine; dvp1977dvp@gmail.com
[2] JSC Motor Sich, Zaporizhzhia, Ukraine; dvirnyk@gmail.com
[3] Instytut Techniczny Wojsk Lotniczych, Warsaw, Poland; radoslaw.przysowa@itwl.pl
* Correspondence: dvp1977dvp@gmail.com
† This paper is an extended version of our paper published in 10th EASN International Conference on Innovation in Aviation & Space to the Satisfaction of the European Citizens.
‡ These authors contributed equally to this work.

Abstract: BACKGROUND: Manufacturing costs, along with operational performance, are among the major factors determining the selection of the propulsion system for unmanned aerial vehicles (UAVs), especially for aerial targets and cruise missiles. OBJECTIVES: In this paper, the design requirements and operating parameters of small turbofan engines for single-use and reusable UAVs are analysed to introduce alternative materials and technologies for manufacturing their compressor blades, such as sintered titanium, a new generation of aluminium and an alloy based on titanium aluminides. METHODS: To assess the influence of severe plastic deformation (SPD) on the hardening efficiency of the proposed materials, the alloys in the coarse-grained and submicrocrystalline states were studied. Changes in physical and mechanical properties of materials were taken into account. The thermodynamic analysis of the compressor was performed in a finite element analysis system (ANSYS) to determine the impact of gas pressure and temperature on the aerodynamic surfaces of compressor blades of all stages. RESULTS: Based on thermal and structural analysis, the stress and temperature maps on compressor blades and vanes were obtained, taking into account the physical and mechanical properties of advanced materials and technologies of their processing. The safety factors of the components were established based on the assessment of their stress-strength reliability. Thanks to nomograms, the possibility of using the new materials and the technologies was confirmed in view of the permissible operating temperature and safety factors of blades. CONCLUSIONS: The proposed alternative materials and production technologies for the compressor blades and vanes meet the design requirements of the turbofan at lower manufacturing costs.

Keywords: turbofan; unmanned aerial vehicles; cruise missile; aerial target; axial compressor; blade; titanium alloy; aluminium alloy; titanium aluminide; safety factor

1. Introduction

Currently, one of the most promising areas in the aerospace and defence industry is the development of unmanned aerial systems for various purposes. They are based on unmanned aerial vehicles (UAVs) of both reusable and single use. Ukrainian and global manufacturers offer gas-turbine engines for UAVs of various types [1–4]. While full-scale turboprops and turbofans, as a rule, are based on engines designed for manned aircraft, small turbofans (Figure 1) have original structure [5–7], which is determined by the tactical and technical characteristics of the platform [8].

Small turbofan engines are designed for reconnaissance UAVs and cruise missiles such as R-360 Neptune, Kite, Kh-55, Tomahawk and Harpoon. The main features of their performance characteristics are a short life cycle (if used as weapons), small size and weight and, as a result, high thrust-to-weight ratio. Also, operation on an unmanned platform contributes to the fact that they are not subject to the aviation safety regulations. Such engines are produced by JSC Motor Sich, SE Ivchenko Progress

Preprints (www.preprints.org) | NOT PEER-REVIEWED | Posted: 10 November 2020 doi:10.20944/preprints202011.0303.v1

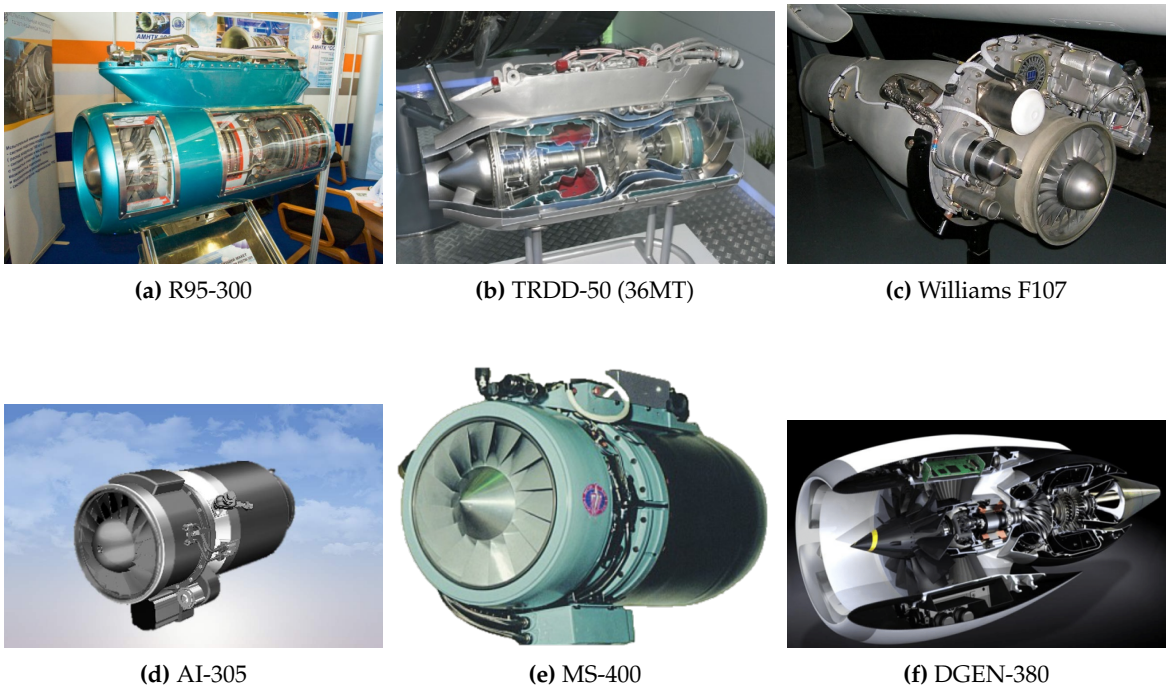

(a) R95-300 **(b)** TRDD-50 (36MT) **(c)** Williams F107

(d) AI-305 **(e)** MS-400 **(f)** DGEN-380

Figure 1. Small turbofan engines

and a number of foreign firms. Engines of this class have thrust in the range of 1.9 - 4 kN, a low bypass ratio and a small dry mass not exceeding 60 - 85 kg. At the same time, to ensure high efficiency, such turbofan engines rotate at several tens of thousands of revolutions per minute, which imposes a number of special requirements on the design of their components and selection of materials. First of all, they should have high specific strength under static loads and a relatively low manufacturing cost. At the same time, their durability, due to the short life cycle and lack of pilot, is secondary to them.

In small turbofan engines both radial and axial compressors are used. Currently, various types of titanium alloys are successfully used to manufacture the blades and vanes of axial compressors [9,10]. The most common are VT6 (Ti-6Al-4V), VT3-1 (Ti-6.7Al-2.5Mo-l.8Cr-0.5Fe-0.25Si) and VT8 (Ti-6.8Al-3.5Mo- 0.32Si). For compressor stages with increased air temperature along the gas path heat-resistant titanium alloys of the VT25 (Ti-6.8Al-2.0Mo-2.0Zr-2.0Sn-l.0W-0.3Si) type are used [11, 12]. For the last stages of the compressor, taking into account the temperature level, heat-resistant nickel-based such as Inconel 718 (EP718-ID) and similar are used. A common drawback of these materials, along with the high cost and energy costs of production, is their poor machinability. Having a combination of properties necessary for the compressor blades of an engine propelling manned aircraft, they are redundant when used on UAVs. This leads to increased cost of engines and UAVs in general. To meet the requirements for UAV power plants, it is necessary to introduce new materials and technologies, which reduce their manufacturing cost.

There are several modern technologies which can be used for manufacturing gas turbines propelling UAVs [13]. When it comes to compressor blades, a number of candidate materials is considered, for example, sintered powder alloys; rare earth aluminium alloys; alloys based on titanium aluminides and others. At present, compressor blades are hardened by laser shock peening [14] which is a surface process which does not modify the inner structure of the alloy. Therefore, to significantly increase the strength and ductility of aircraft materials, severe plastic deformation (SPD) technologies are used [15–18] but the size of produced ingots is still limited. What is more, for each compressor stage, there are a number of limitations both in the operating temperature and mechanical properties which have to be met by introduced materials.

Preprints (www.preprints.org) | NOT PEER-REVIEWED | Posted: 10 November 2020 doi:10.20944/preprints202011.0303.v1

In this work, to reduce the manufacturing cost of a selected small turbofan engine, alternative materials and technologies for producing compressor aerofoils are introduced and evaluated. To ensure structural integrity, the static safety factor is assessed for the blades and vanes of individual stages, taking into account their operating temperature. The main tasks necessary to achieve the goal of work include material selection and strength testing, airflow simulation of the compressor to obtain pressure fields on aerofoil surfaces of all stages and gas temperature, and structural analysis of components to calculate their stress and static safety factor.

2. Materials and methods

2.1. Twist Extrusion

Various SPD methods [19,20] are introduced to improve mechanical, physical, and functional properties of metals and alloys by forming their submicrocrystalline structure [21,22]. Twist extrusion (TE) is a variant of the simple shear deformation process that was introduced by Beygelzimer [23]. Under TE processing, a prismatic billet is extruded through a twist die.

In this work, a number of standard and powder metal alloys (Table 1) sourced from various contractors were processed with TE. The billet (Figure 2) was 70 mm long with the cross-section of 18 × 28 mm. It was placed in a matrix with a helical channel of rectangular cross section with an angle of the helix inclination to the TE axis. The extrusion pressure was FP=1600 MPa for titanium alloys. To increase their plasticity, back pressure BP = 200 MPa was applied to the front end of the billet. To transmit back pressure, a deformable medium was used, which was either a mixture based on the low-melting glass or a copper billet [24].

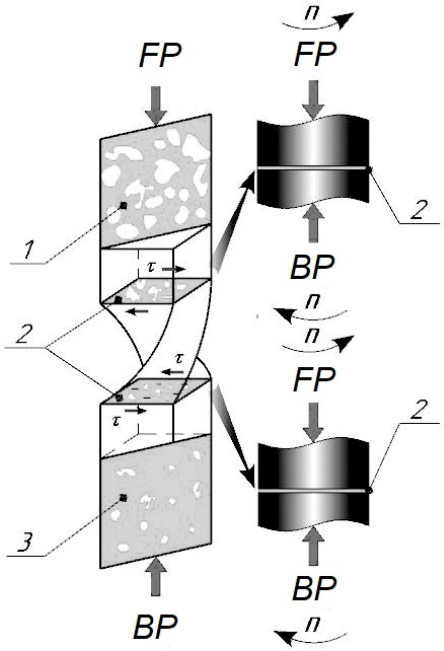

Figure 2. Deformation of a porous billet by twist extrusion: 1 – before TE; 2 - deformation zone; 3 – after TE, FP - forward pressure, BP - back pressure

The total relative shear deformation Λ per pass can be calculated as follows:

$$\Lambda = \frac{2}{\sqrt{3}} \tan \gamma_{max} \quad (1)$$

Preprints (www.preprints.org) | NOT PEER-REVIEWED | Posted: 10 November 2020 doi:10.20944/preprints202011.0303.v1

where γ_{max} is the maximum angle of inclination between the twist line and the extrusion axis. The calculation showed that the total shear deformation per pass is approximately 1.15. Five TE passes were carried out. Thus, the total relative shear deformation of the billet was 5.77.

The average size of the structural components (grains and subgrains) in the samples after five TE passes was in the range of 200 - 500 nm for titanium alloys [25]. The size of the structural components in the original samples was 150 - 300 µm.

2.2. Sintered titanium

One of the known methods of reducing the manufacturing cost of the axial compressor is the use of sintered titanium alloys [26,27] but their residual porosity and low ductility are the reasons that up to now they are used in aircraft engine for a narrow circle of lightly loaded, non-essential components. Therefore, powder materials need consolidation and grain refinement which can be effectively achieved by the SPD process of high-pressure torsion (HPT) [28,29]. However, HPT can produce very small samples which cannot be used to manufacture compressor blades. Therefore, our recent paper [30] uses the physical similarity of the processes occurring in a thin layer of material during HPT and TE to simulate twist extrusion with the available HPT data.

In this work, among others, alloys synthesised from a mixture of selected powder components [31,32] were evaluated. Doping elements (pure Al, Mo and Si metals) were mixed with the matrix titanium powder in a mixer drum at 60–80 rpm to ensure the required chemical composition of the test alloy after sintering. The powders were subjected to single-action compaction in rigid dies at room temperature. The compaction force was 730–760 MPa. The compacts were sintered in vacuum in the range 1250–1270°C with an isothermal holding time of 2.5–3 hours and cooled down in the furnace in vacuum.

Our previous work [33] showed that the characteristics of sintered titanium alloys subjected to SPD in some indicators exceed similar values for regular alloys in cast and deformed states. The preliminary structural analysis of blades made of sintered titanium alloy with subsequent SPD confirmed that their safety margin meets operating conditions [34]. However, an important factor limiting the use of alloys in the compressor design is the elevated temperature caused by air compression in the gas path. Also, given the high rotational speed of the engine, close to 40-50 thousand revolutions per minute, stress analysis results depend heavily on calculated pressure field. As information on the operating temperature and pressure in the compressor stages of small turbofan engines is very limited [35,36], air flow and thermal analysis will be performed in this work.

2.3. Aluminium Alloys and Titanium Aluminides

Aluminium alloys with lithium and scandium are well suited for the use in the turbofan engine, given their high specific strength which exceeds those of titanium alloys [37–39]. Twist extrusion effectively hardens the cast structure of aluminium, so it could be used instead of homogenization annealing [40–42]. However, it is necessary to take into account the operating temperature of components since the heat resistance of aluminium alloys is significantly lower than that of titanium and nickel ones.

Intermetallic Fe_3Al-based alloys could potentially substitute more expensive superalloys and creep-resistant steels. They are characterized by a combination of interesting functional characteristics such as excellent resistance to oxidation, sulfidation and carburizing, good resistance to seawater corrosion, wear, erosion, or cavitation, and high strength to weight ratio [43].

Lightweight, heat-resistant and weldable alloys based on titanium aluminides enable the creation of more efficient compressor designs. These materials offer a number of unique properties: low density, relatively high melting point, high modulus of elasticity, resistance to oxidation and fire, high specific heat resistance, etc. They are well suited for the last stages of compressor blades but their effectiveness is controversial. On one hand, due to the combination of specific strength and heat resistance, they can replace traditional nickel-based alloys [44,45]. On the other hand, the technology

Preprints (www.preprints.org) | NOT PEER-REVIEWED | Posted: 10 November 2020 doi:10.20944/preprints202011.0303.v1

Table 1. Mechanical and physical properties of the alloys considered for compressor aerofoils

Alloy and process	E MPa	ρ kg/m^3	UTS MPa	$\sigma_{0.2}$ MPa	μ	E/ρ 10^6Nm/kg	UTS/ρ 10^6Nm/kg	T_{max} °C
VT8	1.20 E5	4520	980	850	0.30	26.5	0.22	500
VT8_spd	1.08 E5	4400	1250	1150	0.38	24.5	0.28	460
VT8_spk	0.95 E5	4000	700	450	0.10	23.8	0.18	500
VT8_spk_spd	1.10 E5	4400	1040	960	0.32	25.0	0.21	460
Ti-46Al-5Nb-2W	9.50 E4	4200	720	650	0.30	22.6	0.17	750
Ti-46Al-5Nb-2W_spd	8.50 E4	4100	920	880	0.34	20.7	0.22	680
Al 88% Si 9.5%	6.90 E3	2700	75	60	0.33	2.6	0.03	120
Al 88% Si 9.5% _spd	6.20 E3	2680	203	180	0.35	2.3	0.08	100

UTS - ultimate tensile strength, SPD - alloy of a submicrocrystalline structure formed by SPD
SPK (sintered metal powder) - alloy obtained by powder metallurgy methods

of their production and processing is quite energy-intensive, which makes them cost-ineffective in the case of small turbofan engines. While heat explosion is a significantly cheaper technology to synthesise such materials [46], their mechanical properties are not satisfactory for aircraft components, in particular for aero-engines.

In this case, a promising, cost-saving technology for the preparation of semi-finished intermetallic γ-TiAl alloys for aircraft, in particular compressor blades, was a technology based on the methods of self-propagating high-temperature synthesis and subsequent SPD of the initial ingots [47]. Taking into account that this technology not only reduces the cost of manufacturing compressor blades, but also increases the level of their mechanical characteristics, assessing the possibility of their use in the design of engines for UAVs is important.

2.4. Strength testing

To determine the mechanical properties of alloys, 11 mm x 11 mm x 56 mm billets were used to produce standard tensile samples in accordance with GOST 1497-84. Strength testing was carried out on the INSTRON 8802 servohydraulic machine under programmed loading at room and elevated temperature. Five reference samples, serially produced from VT8 alloy bars, were measured to validate the test procedure. The extensometer span was 25 mm. The specimen test portion strain was controlled with an accuracy of 1 µm. The accuracy of stress measurements in the specimen cross-section was $\pm$3 MPa. Extensometer and spring dynamometer readings were ADC-processed and sampled with a rate of Δt=0.01 s [31,48].

Table 1 presents the physical and mechanical properties of considered blade materials. The last column shows that materials after SPD become less heat-resistant because intensive grain grow begins at a lower temperature in their case. The ratio of Young's modulus and material ultimate strength to density characterises the specific stiffness and specific strength of the material. From the point of view of strength, for the production of aircraft engine parts, the most promising materials are those with the maximum values of the specified characteristics. This makes it possible to ensure not only a high level of their strength reliability (safety factor), but also a decrease in the mass of parts. It is known that reducing the mass of the rotor of a gas turbine engine is one of the important directions for improving the design, since it effectively reduces the level of dynamic loads and vibration [49]. However, taking into account that the analysed technologies for obtaining ingots for compressor components (powder metallurgy and severe plastic deformation) lead to a change in the indicated characteristics of materials at the level of 10%, they were not considered as a criterion for choosing a production technology. At the same time, when choosing a material, preference was given to that material, the specific stiffness and strength of which is higher while ensuring equal safety margins.

Preprints (www.preprints.org) | NOT PEER-REVIEWED | Posted: 10 November 2020 doi:10.20944/preprints202011.0303.v1

2.5. Modelling the compressor

The effectiveness of the use of candidate materials for manufacturing blades and vanes was evaluated for an axial compressor having the geometry representative for small turbofan engines. The stress-strain state of compressor blades was estimated by a coupled Finite Element Analysis, which included a flow calculation to determine the pressure field and a direct strength calculation to determine the field of acting forces [50–52]. The analysis was performed for a 6-stage axial compressor (Figure 3). The fan was not considered in this work as its blades are too large for SPD technology and also sintered alloys does not provide the necessary level of strength.

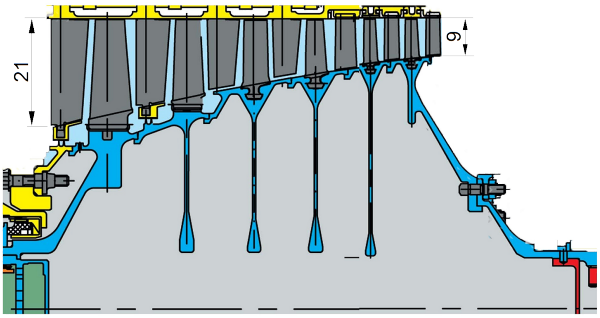

Figure 3. Axial compressor

The section profile of the first compressor stage is shown in Figure 4. The compressor profile of the compressor blades corresponded to the standard aerodynamic profile of NACA 7404 - 7405 AIRFOIL. The total number of blades for the compressor stages is given in Table 2.

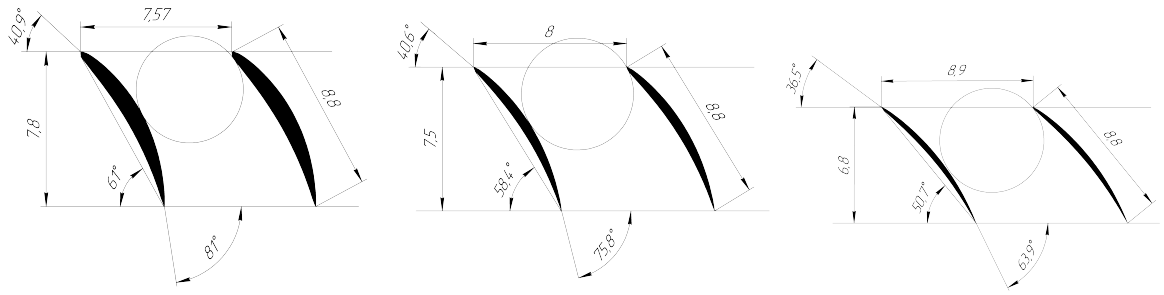

(a) lower section **(b)** midspan **(c)** tip section

Figure 4. Profile of the first stage blade

Table 2. Number of compressor blades

Compressor stage	R1	R2	R3	R4	R5	R6
Number of blades	37	43	59	67	73	81

Using the Unigraphics NX system, models of blades and vanes (one pair per each stage) and inlet guide vanes (IGV) were built. To develop the aerofoil profile, the surface modelling method was used, while for roots, the method based on Boolean operations with geometric primitives (Figure 5). To create finite element models, an ICEM CFD grid generator was used. The mesh models of the blades consisted of 15,000 - 18,000 hexagonal SOLID 186 elements. ANSYS Workbench version 2019 R3 was used for the calculations. Blades were fixed at the root plane.

Preprints (www.preprints.org) | NOT PEER-REVIEWED | Posted: 10 November 2020 doi:10.20944/preprints202011.0303.v1

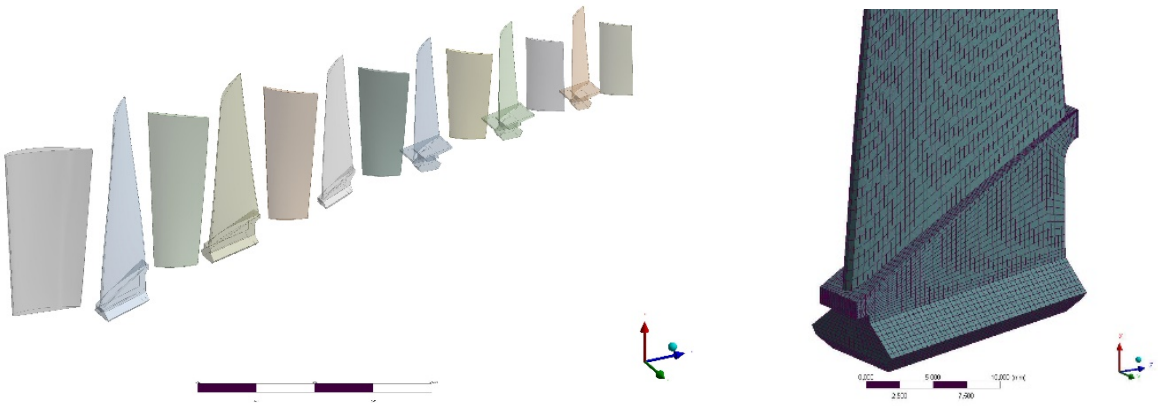

(a) compressor aerofoils **(b)** 1st stage blade root

Figure 5. Structural model

2.6. CFD model

Temperature along the compressor gas path and pressure on the aerodynamic surfaces of the blades was determined by flow calculation in Ansys CFX with the finite element method. CFD model of the compressor inter-blade channel was obtained by arranging the domains of each compressor stage in the axial and radial directions. To build a mesh of the compressor flow, the TurboGrid grid generator was used (Figure 6). Volumetric finite elements intended for CFD calculations were used. To reduce the required computing power, one blade was modelled for each compressor stage with the cyclic symmetry along the boundaries of the domain (Figure 6c). The boundary conditions were set in the form of total inlet pressure, airflow at the compressor outlet, and rotational speed. (Figure 6d).

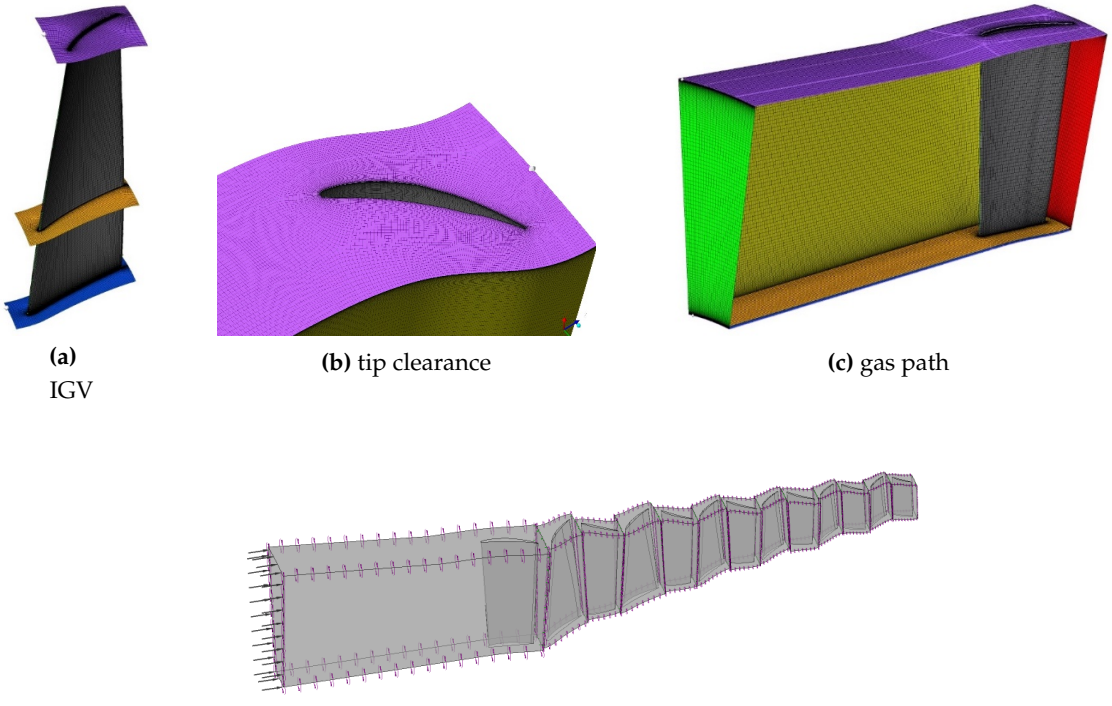

(a) IGV **(b)** tip clearance **(c)** gas path

(d) boundary conditions

Figure 6. Airflow model of the compressor

Preprints (www.preprints.org) | NOT PEER-REVIEWED | Posted: 10 November 2020 doi:10.20944/preprints202011.0303.v1

An interface between stationary and rotating regions (Stage Mizing-Plane) was defined on the mating boundaries of regions belonging to different steps, which allows for the interpolation between mating grids. A satisfactory criterion for the convergence of the calculation was the value of the mean square residual at the level of 10^{-6}. This convergence was achieved at 1200 - 1400 iterations. We used the SST $k-\omega$ model of turbulence [53,54], as the most accurate and reliable for flows with a positive pressure gradient when flowing around profiles. At the inlet and outlet of the compressor, the mass flow rate and temperature were set corresponding to the emergency operation of the compressor. The the simulation results were validated according to the methodology described in [55].

2.7. Structural analysis

To assess the stress-strain state of the blade and temperature distribution, a structural analysis was performed fed with the results of the flow calculation. The aerodynamic surfaces of the blades (pressure and suction sides) were loaded with the pressure and temperature fields obtained as a result of preliminary flow calculation.

Typically, both static and fatigue strength is evaluated for new components [56,57]. However, to calculate the safety factor, one needs material data such as the endurance limit of laboratory samples at operating temperature, the amplitude of alternating stress at the time of failure, as well as the effective coefficient of stress concentration and the magnitude of their variation. Considering that when analysing the suitability of new materials, these data were not available, the static safety factor (SF) was evaluated with the well known formula:

$$SF = \frac{\sigma_{0.2}}{\sigma_{Mises}} \tag{2}$$

Where $\sigma_{0.2}$ - conditional yield strength of the blade material, σ_{Mises}- maximum value of the von Mises stress in the compressor blades

3. Results and discussion

Figure 7 shows the calculated pressure fields on blade surfaces, and the flow temperature. The flow temperature was used as the initial data for thermal analysis as the boundary condition of the third kind to calculate the surface temperature of blades (8). The obtained operating temperature of the compressor blades makes it possible to evaluate the suitability of the considered materials. Given that the blade has a relatively small profile thickness, the temperature distribution over the cross-section was considered uniform.

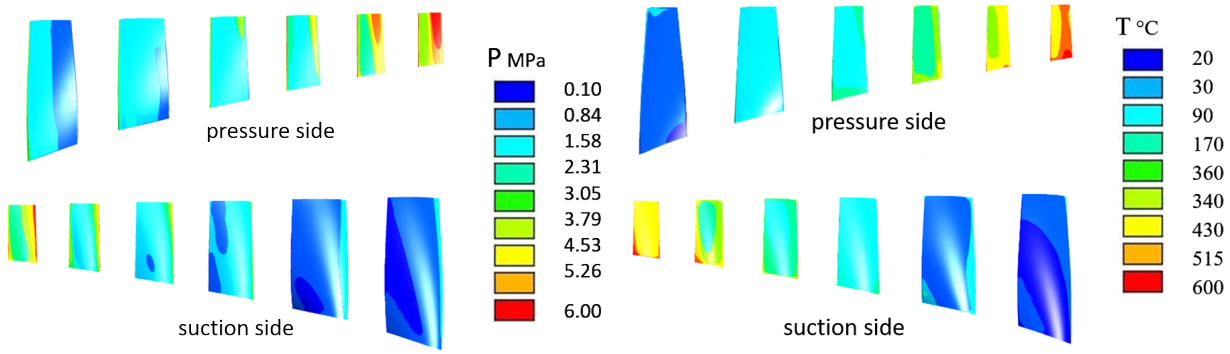

(e) pressure field **(f)** temperature field

Figure 7. Pressure and temperature field on blade surfaces

Preprints (www.preprints.org) | NOT PEER-REVIEWED | Posted: 10 November 2020 doi:10.20944/preprints202011.0303.v1

Table 3. Equivalent stress and static safety factor of blades made from candidate materials

Rotor stage	R1		R2		R3		R4		R5		R6	
Alloy/process	σ_{max} MPa	SF	σ_{max} MPa	SF	σ_{max} MPa	SF	σ_{max} MPa	SF	σ_{max} MPa	SF	σ_{max} MPa	SF
VT8	480.2	1.77	481.1	1.77	805.8	1.05	893.3	0.95	717.6	1.19	864.5	0.98
VT8_spd	481.9	2.39	451.6	2.25	802.4	1.43	859.4	1.34	718.4	1.60	889.4	1.29
VT8_spk	477.2	0.94	517.3	0.87	801.2	0.56	938.6	0.48	719.9	0.63	882.2	0.51
VT8_spk_spd	481.7	1.99	474.2	2.02	804.3	1.91	886.0	1.08	717.4	1.33	872.2	1.10
TiAl	483.6	1.34	473.6	1.37	803.1	0.81	892.3	0.73	717.2	0.91	873.5	0.74
TiAl_spd	483.6	1.82	462.9	1.90	801.3	1.10	877.3	1.00	717.5	1.23	885.5	0.99
Al 88 Si 9.5	460.0	0.13	451.1	0.13	789.8	0.08	877.0	0.07	717.0	0.08	922.4	0.07
Al 88 Si 9.5_spd	460.0	0.39	450.9	0.40	789.0	0.23	868.7	0.21	717.3	0.25	928.3	0.19

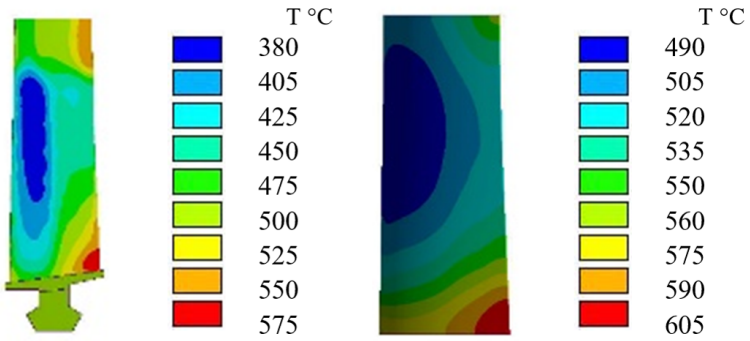

Figure 8. Temperature field for blades and vanes of stage 6

Calculated stress distribution in the aerofoils (Figure 9) made it possible to evaluate candidate materials and processing technologies in view of their structural integrity. Values of maximum equivalent stress and static safety factor of blades and vanes made from advanced materials and technologies are given in Table 3 and 4. Materials with safety factor less than the threshold of 1.1 or 1.15 cannot be used in the particular stage [58]. This value was selected by the manufacturer on the basis of industrial experience and reliability data. Under certain conditions, such a low SF threshold is acceptable in aircraft components, especially for unmanned and single-use platforms.

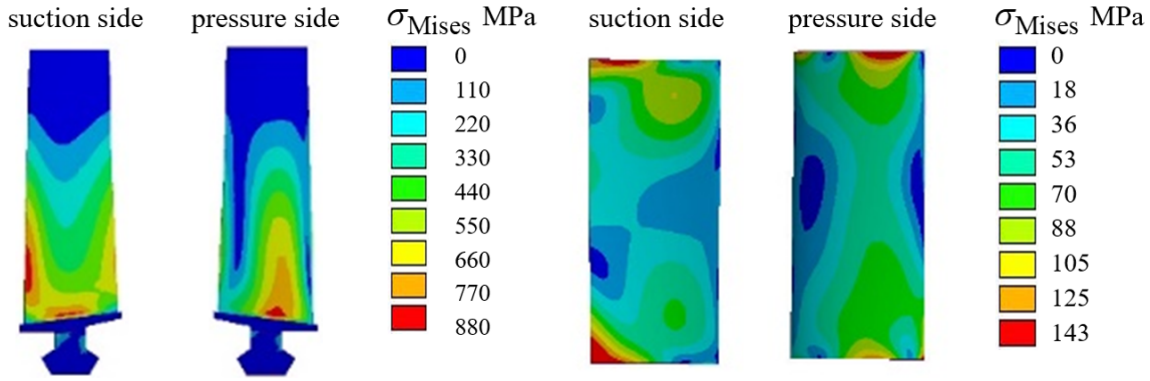

Figure 9. von Misses stress in blades and vanes made from VT8_spk_spd alloy in engine emergency mode

Analysing the obtained data, we can conclude that the candidate materials and processing technologies can be used for manufacturing compressor blades. Considering that the analysis of the application area of titanium alloys by the criterion of temperature and strength is complicated due to the variety of technologies used for their preparation and processing, nomograms were developed for this purpose (Figure 10). Thus, for blades, VT8 alloy is limited to rotor stages 1-2 in terms of their

Preprints (www.preprints.org) | NOT PEER-REVIEWED | Posted: 10 November 2020 doi:10.20944/preprints202011.0303.v1

Table 4. Equivalent stress and static safety factor of vanes made from candidate materials

Stator stage	S1		S2		S3		S4		S5		S6	
Alloy/process	σ_{max} MPa	SF	σ_{max} MPa	SF	σ_{max} MPa	SF	σ_{max} MPa	SF	σ_{max} MPa	SF	σ_{max} MPa	SF
VT8	8.8	96.2	45.5	18.7	54.0	15.8	133.5	6.4	140.6	6.1	142.4	6.0
VT8_spd	8.9	129.7	43.6	26.4	53.8	21.4	128.4	9.0	140.8	8.2	146.5	7.9
VT8_spk	8.8	51.3	48.9	9.2	53.7	8.4	140.2	3.2	141.1	3.2	145.3	3.1
VT8_spk_spd	8.8	84.6	44.8	16.7	53.9	13.9	132.4	5.7	140.6	5.3	143.6	5.2
TiAl	8.9	73.0	44.8	14.5	53.8	12.1	133.3	4.9	140.5	4.6	143.8	4.5
TiAl_spd	8.9	98.9	43.7	20.1	53.7	16.4	131.1	6.7	140.6	6.3	145.8	6.0
Al 88 Si 9.5	8.5	7.1	42.6	1.4	52.9	1.1	131.0	0.5	140.5	0.4	151.9	0.4
Al 88 Si 9.5_spd	8.5	21.3	42.6	4.2	52.9	3.4	129.8	1.4	140.6	1.3	152.9	1.2

strength reliability (Figure 10a). The use of SPD methods expands the scope of its application up to the 7^{th} stage; however, in terms of the level of the thermal state, VT8 usage is limited to blades of the first five stages.

From these nomograms it can be inferred that strength of the blades of all compressor stages, made of titanium alloy in the sintered state, is below the acceptable threshold (1.1 - 1.15). Therefore they cannot be used, despite the significantly lower manufacturing cost in comparison with an alloy in a deformed state. However, the use of SPD methods, due to the elimination of porosity, the formation of a submicrocrystalline structure in the entire cross-section and the homogenization of alloying elements, contributes to a significant increase in strength and, as a consequence, the expansion of their application at all stages .

At the same time, the operating temperature of the alloy in the submicrocrystalline state is lower than one in its standard form which does not allow for their use in 6^{th} stage blades (Figure 10a). Considering that the compressor stator vanes experience a load only from the flow, the field of application of the VT8 alloy is limited only by its operating temperature, regardless of the technology of production and processing (Figure 10b). Despite the great strength, the sintered VT8 alloy synthesized from a mixture of powder components and subjected to severe plastic deformation, in comparison with the sintered alloy, has a smaller range of application due to the lower operating temperature. Taking into account the lower cost of obtaining sintered titanium alloys, it can be argued that for the 5^{th} stage blades, their use is the most rational.

Alloys based on aluminium with a coarse-grained and submicrocrystalline structure according to the thermal criterion can be applied only to blades of the first and second stages. However, a safety factor assessment indicates that their applications are limited by stator vanes. At the same time, the use of modern aluminium alloys as the material for the blades is possible without the use of additional pressure processing technologies, which reduces the cost of their production. Given the low weight and cost of blades made of aluminium alloy compared to titanium blades, their use can be considered justified. Moreover, the well-known problems of such alloys as, for example, low hardness and resistance to sand erosion, are an uncritical factor for UAV engines.

Alloys based on titanium aluminides are the most heat resistant of the considered ones, which predetermines their use for manufacturing blades of the last compressor stages. From the point of view of the permissible operating temperature, this alloy can be applied to blades of all stages regardless of their structural state (Tables 1, 3, 4). At the same time, from the point of view of strength reliability for blades, their use is allowed up to stage 3 without additional strain hardening and up to 4^{th} stage with processing by SPD methods (Table 3).

For all stator stages, the safety factor of vanes made from titanium aluminides is higher than the threshold regardless of the use of SPD (Table 4). Thus, this alloy is used for manufacturing vanes of stages 5 and 6, for which, due to temperature limitations, lighter titanium alloys may not be applicable. Nevertheless, the replacement of more heat-resistant Inconel 718 alloys with titanium aluminides will reduce the weight of gas turbine engines.

Preprints (www.preprints.org) | NOT PEER-REVIEWED | Posted: 10 November 2020 doi:10.20944/preprints202011.0303.v1

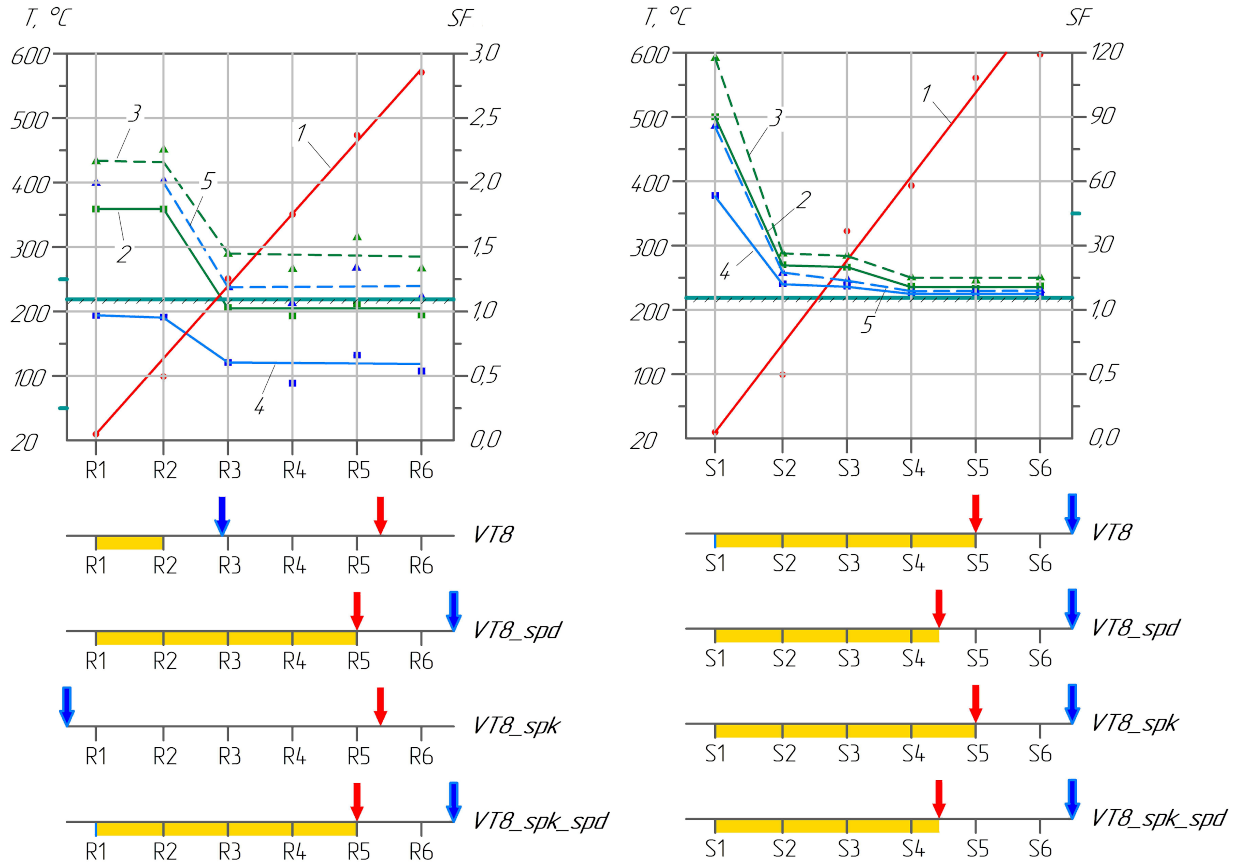

(a) blades **(b)** vanes

Figure 10. Nomogram of temperature limit and safety factor of aerofoils made from VT8 titanium alloy: 1 - temperature °C; 2 - VT8; 3 - VT8_spd; 4 - VT8_spk; 5 - VT8_spk_spd

It should be noted that the considered limitations associated with the temperature state of alloys in the submicrocrystalline state are determined based on the conditions of the onset of recrystallization processes. Considering that recrystallization processes take a relatively long time, exceeding the flight cycle of single-use UAVs (cruise missiles, disposable reconnaissance vehicles, aerial targets, etc.), this restriction can be removed for such turbofan engines. In this case, their use in terms of the maximum allowable temperature will be similar to alloys in a coarse-crystalline state. The calculated values of the safety factors for compressor components made from considered alloys and technologies let us propose their field of application (Figure 11).

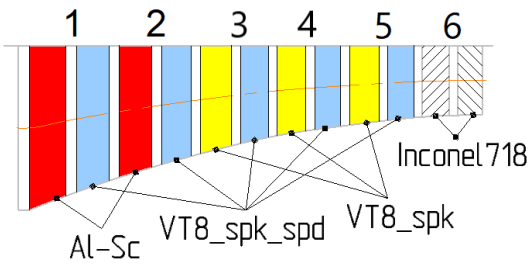

Figure 11. Field of application of alloys and their processing technologies in the compressor

4. Conclusions

The analysis of the thermal and stress-strain state of the compressor blades and vanes of the small turbofan used as the main engine for UAVs, in combination with the tensile testing of the candidate alloys, made it possible to develop recommendations for their use:

1. It was found that the vanes of the first fifth stator stages can be made of sintered VT8 titanium alloy without strain hardening. Respectively, the blades of the first fifth rotor stages can be made of sintered VT8 titanium alloy, subjected to SPD processing.
2. An aluminium alloy of the Al88-Si9.5 type, regardless of the use of SPD, can be used to make vanes of S1-S2.
3. An alloy based on titanium aluminides of the Ti-46Al-5Nb-2W type can be used for 5^{th}-stage blades after processing with SPD methods. Given the possibility of using VT8 titanium alloy for these blades and the insufficient strength reliability of 6^{th}-stage blades made from it, its use in the design of a small turbofan engine is irrational.

Taking into account that the change in the physical and mechanical properties of materials can affect not only the stress-strain state of the blades but also their dynamic characteristics, at the next stage of research, it is rational to assess the effect of the material and its production technologies on the natural frequencies of the blades. For the engines under study, Campbell diagrams will be produced and the surge margin of the compressor predicted. Also, the damping properties of alloys in various conditions should be analysed.

Acknowledgements

We would like to thank Dr Wieslaw Beres and Prof. Sylwester Klysz for their comments on an earlier version of the manuscript, although any errors are our own and should not tarnish the reputations of these esteemed persons.

References

1. Telesyk. Motor Sich engines for UAVs (Dvigateli "Motor Sich" dlja BPLA). https://telesyk.livejournal.com/146218.html, accessed on 02.11.2020.
2. Brand, J.H.; Dooley, K.A.; Dowhan, M.J.; Walters, C. More Electric Small Turbofan. General Aviation Technology Conference & Exhibition; , 2004; Number 724. doi:10.4271/2004-01-1804.
3. Brooks, V.E. Small Turbine Engine Evolution. *SAE International Journal of Aerospace* **2008**, *1*, 2008–01–2874. doi:10.4271/2008-01-2874.
4. Costa, F.P.; Henrique, L.; Whitacker, L.; Bringhenti, C.; Tomita, J.T. An overview of small gas turbine engines. ISABE-2019-24387; , 2019; Number November.
5. Weinberg, M.; Wyzykowski, J. Development and Testing of a Commercial Turbofan Engine for High Altitude UAV Applications. SAE Technical Papers, 2001, number 724. doi:10.4271/2001-01-2972.
6. Rodgers, C. Affordable Smaller Turbofans. Volume 1: Turbo Expo 2005. ASMEDC, 2005, Vol. 1, pp. 1–10. doi:10.1115/GT2005-68042.
7. Large, J.; Pesyridis, A. Investigation of micro gas turbine systems for high speed long loiter tactical unmanned air systems. *Aerospace* **2019**, *6*. doi:10.3390/AEROSPACE6050055.
8. Nelson, J.R.; Dix, D.M. Development of Engines for Unmanned Air Vehicles: Some Factors to be Considered. Technical Report January, OSD or Non-Service DoD Agency, 2003. doi:10.21236/ADA412680.
9. Moiseev, V.N. Titanium in Russia. *Metal Science and Heat Treatment* **2005**, *47*, 371–376. doi:10.1007/s11041-005-0080-9.
10. Pavlova, T.; Kashapov, O.; Nochovnaja, N. Titanovye splavy dlja gazoturbinnyh dvigatelej (Titanium alloys for gas turbine engines). *Proceedings of VIAM* **2012**, *5*, 8–14.
11. Kashapov, O.; Novak, A.; Nochovnaya, N.; Pavlova, T. State, problems and prospects of heat-resistant titanium alloys for GTE parts. *Proceedings of VIAM* **2013**, *3*.

12. Whittaker, M. Titanium in the Gas Turbine Engine. In *Advances in Gas Turbine Technology*; Benini, E., Ed.; InTech, 2011; Vol. 4. doi:10.5772/21524.
13. Moustapha, H. Future Technology Challenges for Small Gas Turbines. AIAA International Air and Space Symposium and Exposition: The Next 100 Years; American Institute of Aeronautics and Astronautics: Reston, Virigina, 2003; Number July 2003, pp. 1–11. doi:10.2514/6.2003-2559.
14. Zou, S.; Wu, J.; Zhang, Y.; Gong, S.; Sun, G.; Ni, Z.; Cao, Z.; Che, Z.; Feng, A. Surface integrity and fatigue lives of Ti17 compressor blades subjected to laser shock peening with square spots. *Surface and Coatings Technology* **2018**, *347*, 398–406. doi:10.1016/j.surfcoat.2018.05.023.
15. Azushima, A.; Kopp, R.; Korhonen, A.; Yang, D.Y.; Micari, F.; Lahoti, G.D.; Groche, P.; Yanagimoto, J.; Tsuji, N.; Rosochowski, A.; Yanagida, A. Severe plastic deformation (SPD) processes for metals. *CIRP Annals - Manufacturing Technology* **2008**, *57*, 716–735. doi:10.1016/j.cirp.2008.09.005.
16. Kommel, L. Microstructure evolution in titanium alloys enforced by joule heating and severe plastic deformation concurrently. *Journal of Manufacturing Technology Research* **2010**, *2*, 59–75.
17. Valiev, R.Z.; Estrin, Y.; Horita, Z.; Langdon, T.G.; Zehetbauer, M.J.; Zhu, Y. Producing Bulk Ultrafine-Grained Materials by Severe Plastic Deformation: Ten Years Later. *JOM* **2016**, *68*, 1216–1226. doi:10.1007/s11837-016-1820-6.
18. Łyszkowski, R.; Polkowski, W.; Czujko, T. Severe plastic deformation of Fe-22Al-5Cr alloy by cross-channel extrusion with back pressure. *Materials* **2018**, *11*, 1–17. doi:10.3390/ma11112214.
19. Estrin, Y.; Vinogradov, A. Extreme grain refinement by severe plastic deformation: A wealth of challenging science. *Acta Materialia* **2013**, *61*, 782–817. doi:10.1016/j.actamat.2012.10.038.
20. Semenova, I.P.; Raab, G.I.; Valiev, R.Z. Nanostructured titanium alloys: New developments and application prospects. *Nanotechnologies in Russia* **2014**, *9*, 311–324. doi:10.1134/S199507801403015X.
21. Pavlenko, D.V.; Beygelzimer, Y.E. Vortices in Noncompact Blanks During Twist Extrusion. *Powder Metallurgy and Metal Ceramics* **2016**, *54*, 517–524. doi:10.1007/s11106-016-9744-9.
22. Bahadori, S.R.; Mousavi, S.A.A.A.; Shahab, A.R. Sequence effects of twist extrusion and rolling on microstructure and mechanical properties of aluminum alloy 8112. *Journal of Physics: Conference Series* **2010**, *240*, 012132. doi:10.1088/1742-6596/240/1/012132.
23. Beygelzimer, Y.E.; Orlov, D.; Korshunov, A.; Synkov, S.; Varyukhin, V.; Vedernikova, I.; Reshetov, A.; Synkov, A.; Polyakov, L.; Korotchenkova, I. Features of twist extrusion: Method, structures & material properties. *Solid State Phenomena* **2006**, *114*, 69–78. doi:10.4028/www.scientific.net/SSP.114.69.
24. Beygelzimer, Y.; Kulagin, R.; Estrin, Y.; Toth, L.S.; Kim, H.S.; Latypov, M.I. Twist Extrusion as a Potent Tool for Obtaining Advanced Engineering Materials: A Review. *Advanced Engineering Materials* **2017**, *19*. doi:10.1002/adem.201600873.
25. Pavlenko, D.V. Effect of Porosity Parameters on the Strength of Gas Turbine Compressor Blades Made of Titanium Alloys. *Strength of Materials* **2019**, *51*, 887–899. doi:10.1007/s11223-020-00139-0.
26. Ivasishin, O.M.; Anokhin, V.M.; Demidik, A.N.; Sawakin, D.G. Cost-effective blended elemental powder metallurgy of titanium alloys for transportation application. *Key Engineering Materials* **2000**, *188*, 55–62. doi:10.4028/www.scientific.net/kem.188.55.
27. Fang, Z.Z.; Sun, P. Pathways to optimize performance/cost ratio of powder metallurgy titanium - A perspective. *Key Engineering Materials* **2012**, *520*, 15–23. doi:10.4028/www.scientific.net/KEM.520.15.
28. Pavlenko, D. Povyshenie tehnologicheskoj plastichnosti spechennyh titanovyh splavov (Improving the technological plasticity of sintered titanium alloys). *The processes of mechanical processing in machine building* **2015**, pp. 102–112.
29. Kulagin, R.; Zhao, Y.; Beygelzimer, Y.; Toth.; S., L.; Shtern, M. Modeling strain and density distributions during high-pressure torsion of pre-compacted powder materials. *Materials Research Letters* **2017**, *5*, 179–186. doi:10.1080/21663831.2016.1241318.
30. Pavlenko, D. Structural and chemical inhomogeneities in the sintered titanium alloys after severe plastic deformation. *Metaloznavstvo ta obrobka metalìv* **2020**, *95*, 37–45. doi:10.15407/mom2020.03.037.
31. Bykov, I.O.; Ovchinnikov, A.V.; Pavlenko, D.V.; Lechovitzer, Z.V. Composition, Structure, and Properties of Sintered Silicon-Containing Titanium Alloys. *Powder Metallurgy and Metal Ceramics* **2020**, *58*, 613–621. doi:10.1007/s11106-020-00117-w.

32. Beygelzimer, Y.E.; Pavlenko, D.V.; Synkov, O.S.; Davydenko, O.O. The Efficiency of Twist Extrusion for Compaction of Powder Materials. *Powder Metallurgy and Metal Ceramics* **2019**, *58*, 7–12. doi:10.1007/s11106-019-00041-8.
33. Pavlenko, D.V.; Ovchinnikov, A.V. Effect of Deformation by the Method of Screw Extrusion on the Structure and Properties of V?1-0 Alloy in Different States. *Materials Science* **2015**, *51*, 52–60. doi:10.1007/s11003-015-9809-9.
34. Pavlenko, D.V.; Pribora, T.I.; Kocjuba, V.J.; Paholka, S.N. Perspektivnye materialy i tehnologii dlja detalej rotora kompressora GTD (Promising materials and technologies for the rotating components of axial compressor). *Aerospace Science and Technology* **2016**, *8*, 128–138.
35. Lu, W.; Huang, G.; Xiang, X.; Wang, J.; Yang, Y. Thermodynamic and aerodynamic analysis of an air-driven fan system in low-cost high-bypass-ratio turbofan engine. *Energies* **2019**, *12*. doi:10.3390/en12101917.
36. Chivukula, V.; Mohla, R.; Srinivas, G. The flow visualization of small-scale aircraft engine axial flow turbine rotor using numerical technique. *International Journal of Mechanical and Production Engineering Research and Development* **2019**, *9*, 777–784. doi:10.24247/ijmperdaug201978.
37. Zakharov, V. Effect of Scandium on the Structure and Properties of Aluminum Alloys. *Metal Science and Heat Treatment* **2003**, *45*, 246–253. doi:10.1023/A:1027368032062.
38. Røyset, J.; Ryum, N. Scandium in aluminium alloys. *International Materials Reviews* **2005**, *50*, 19–44. doi:10.1179/174328005X14311.
39. Ahmad, Z. The properties and application of scandium-reinforced aluminum. *Jom* **2003**, *55*, 35–39. doi:10.1007/s11837-003-0224-6.
40. Liddicoat, P.V.; Liao, X.Z.; Zhao, Y.; Zhu, Y.; Murashkin, M.Y.; Lavernia, E.J.; Valiev, R.Z.; Ringer, S.P. Nanostructural hierarchy increases the strength of aluminium alloys. *Nature Communications* **2010**. doi:10.1038/ncomms1062.
41. Beygelzimer, Y.; Kulagin, R.; Raspornya, D.; Varukhin, D. Deformation homogenization of aluminum alloys through twist extrusion. 10th Int. Conf. Techn. Plast. (ICTP 2011); , 2011; pp. 241–243.
42. Seikh, A.H.; Baig, M.; Ur Rehman, A. Effect of Severe Plastic Deformation, through Equal-Channel Angular Press Processing, on the Electrochemical Behavior of Al5083 Alloy. *Applied Sciences* **2020**, *10*, 7776. doi:10.3390/app10217776.
43. Łyszkowski, R.; Czujko, T.; Varin, R.A. Multi-axial forging of Fe3Al-base intermetallic alloy and its mechanical properties. *Journal of Materials Science* **2017**, *52*, 2902–2914. doi:10.1007/s10853-016-0584-2.
44. Nochovnaya, N.A.; Panin, P.V.; Kochetkov, A.S.; Bokov, K.A. Modern Refractory Alloys Based on Titanium Gamma-Aluminide: Prospects of Development and Application. *Metal Science and Heat Treatment* **2014**, *56*, 364–367. doi:10.1007/s11041-014-9763-4.
45. Imayev, V.; Imayev, R.; Gaisin, R.; Nazarova, T.; Shagiev, M.; Mulyukov, R. Heat-resistant intermetallic alloys and composites based on titanium: microstructure, mechanical properties and possible application. *Materials Physics and Mechanics* **2017**, *33(1)*, 80–96. doi:10.18720/MPM.3312017_9.
46. Belokon, K.; Belokon, Y. The Usage of Heat Explosion to Synthesize Intermetallic Compounds and Alloys. In *Processing, Properties, and Design of Advanced Ceramics and Composites II: Ceramic Transactions, Volume 261*; The American Ceramic Society, 2018; pp. 109–115. doi:10.1002/9781119423829.ch9.
47. Pavlenko, D.V.; Belokon', Y.; Tkach, D.V. Resource-Saving Technology of Manufacturing of Semifinished Products from Intermetallic γ-TiAl Alloys Intended for Aviation Engineering. *Materials Science* **2020**, *55*, 118–124. doi:10.1007/s11003-020-00386-1.
48. Karpinos, B.S.; Pavlenko, D.V.; Kachan, O.Y. Deformation of a submicrocrystalline VT1-0 titanium alloy under static loading. *Strength of Materials* **2012**, *44*, 100–107. doi:10.1007/s11223-012-9354-9.
49. Przysowa, R.; Russhard, P. Non-Contact Measurement of Blade Vibration in an Axial Compressor. *Sensors* **2020**, *20*, 68. doi:10.3390/s20010068.
50. Masud, J.; Ahmed, S. Design Refinement and Performance Analysis of Two-Stage Fan for Small Turbofan Engines. 45th AIAA Aerospace Sciences Meeting and Exhibit; American Institute of Aeronautics and Astronautics: Reston, Virigina, 2007; Vol. 1, pp. 161–168. doi:10.2514/6.2007-23.
51. Patel, K.S.; Ranjan, R.; Maruthi, N.H.; Deshpande, S.M.; Narasimha, R. Predictions of aero-thermal loading of an HPT stator blade of a typical small turbofan engine Turbomachinery Flows. 19 th AeSI Annual CFD Symposium; , 2017.

52. Rehman, M.; Afzal, R. Design and analysis of a 11:1 centrifugal compressor for a small turbofan engine. 2019 16th International Bhurban Conference on Applied Sciences and Technology (IBCAST). IEEE, 2019, pp. 189–196. doi:10.1109/IBCAST.2019.8667249.
53. Evans, S.; Lardeau, S. Validation of a turbulence methodology using the SST k-ω model for adjoint calculation. 54th AIAA Aerospace Sciences Meeting; American Institute of Aeronautics and Astronautics: Reston, Virginia, 2016; Number August. doi:10.2514/6.2016-0585.
54. Piovesan, T.; Magrini, A.; Benini, E. Accurate 2-D modelling of transonic compressor cascade aerodynamics. *Aerospace* **2019**, *6*, 1–19. doi:10.3390/AEROSPACE6050057.
55. Dvirnyk, Y.; Pavlenko, D.; Przysowa, R. Determination of Serviceability Limits of a Turboshaft Engine by the Criterion of Blade Natural Frequency and Stall Margin. *Aerospace* **2019**, *6*, 132. doi:10.3390/aerospace6120132.
56. Będkowski, W. Assessment of the fatigue life of machine components under service loading - A review of selected problems. *Journal of Theoretical and Applied Mechanics (Poland)* **2014**, *52*, 443–458.
57. Mehdizadeh, O.; Zhang, C.; Shi, F. Flow-Induced Vibratory Stress Prediction on Small Turbofan Engine Compressor Vanes Using Fluid-Structure Interaction Analysis. 44th AIAA/ASME/SAE/ASEE Joint Propulsion Conference & Exhibit; American Institute of Aeronautics and Astronautics: Reston, Virigina, 2008; Number July, pp. 1–8. doi:10.2514/6.2008-4744.
58. Mulville, D.R. Structural design and test factors of safety for spaceflight hardware. Technical report, Technical Report NASA-STD-5001, NASA, 1996.